CHEMISTRY OF MATERIALS

Article

pubs.acs.org/cm

Two Are Better than One: Bidentate Adsorbates Offer Precise Control of Interfacial Composition and Properties

Han Ju Lee, Andrew C. Jamison, and T. Randall Lee*

Department of Chemistry and the Texas Center for Superconductivity, University of Houston, 4800 Calhoun Road, Houston, Texas 77204-5003, United States

Supporting Information

ABSTRACT: Mixed self-assembled monolayers (SAMs) generated from perfluoro-, *n*-alkyl-, and oligo(ethylene glycol)-terminated alkanedithiols were utilized to prepare two-dimensional interfaces with precise composition and wettability. Interfacial control was afforded simply by adjusting the mole fraction of the adsorbates present in the development solutions and was modulated by the dual contributions of the tailgroups of the bidentate thiols. In contrast, the composition and wettability of mixed SAMs generated from traditional monodentate thiols bearing analogous tailgroups failed to track systematically with the mole fractions of the adsorbates in the development solutions, reflecting a greater dependence on solvent/adsorbate interactions. All of the SAMs were thoroughly characterized by contact angle goniometry, ellipsometry, X-ray photoelectron spectroscopy (XPS), and polarization modulation infrared reflection−absorption spectroscopy (PM-IRRAS). Furthermore, solution-phase displacement tests performed to evaluate the stability of the adsorbates as a function of the adsorbate composition of the mixed alkanedithiolate films, provided evidence of the markedly enhanced stability associated with mixed SAMs formed from bidentate adsorbates.

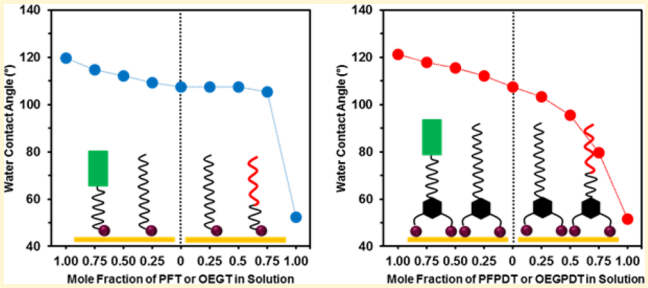

INTRODUCTION

The wettability of materials is affected by surface physical and chemical properties, such as interfacial morphology and the nature of the surface functional groups.[1−16] To control wettability, researchers have developed nanostructures generated, for example, from the alignment of carbon nanotubes,[1] through the microcontact printing of polymers,[2] and by templating particle assemblies.[3] Numerous techniques for generating surfaces with defined interfacial functional groups have been developed to control the wettability of solid surfaces. For example, Lee and co-workers have demonstrated that the hydrophobic surfaces of polystyrene fibers can be converted into hydrophilic surfaces by deposition of titanium oxide nanoparticles onto these surfaces.[6] Furthermore, the degree of hydrophilicity was successfully controlled by ultraviolet light illumination—a process that generates OH^- radicals from water and Ti^{3+} on the surface of the particles, increasing the presence of adsorbed water. Plasma treatment has also been used for the generation of surface functional groups. Pakdel and co-workers generated hydroxyl groups on boron nitride nanostructured films using air-plasma treatment.[7] Alternatively, a number of systems incorporating polymer coatings have been developed for the control of surface wettability.[8−10] Pei and co-workers prepared surface-grafted polymer brushes with poly(3-(methacryloylamido)propyl-*N*,*N*′-dimethyl(3-sulfopropyl)-ammonium hydroxide) (PMPDSAH) and poly(methyl methacrylate)-*b*-PMPDSAH from initiators bound to a poly(pyrrole-*co*-pyrrolyl butyric acid) film (an electrochemically active conducting polymer; ECP) on glassy carbon substrates.[9] The wettability of these environmentally sensitive polymer brushes could be switched electrochemically through changes in the oxidation state of the ECP, thereby changing the ionic content within the polymer brushes, leading to transitions in their conformational order and interfacial wettability. Finally, and perhaps most ubiquitously, many researchers have used self-assembled molecular films to control surface wettability.[11−16] Self-assembled monolayers (SAMs) have proven to be a reliable and convenient technology for modifying the surfaces of metals and various oxides.[17−19]

Dynamic and reversible control of wettability on the surfaces of SAMs have been accomplished by a variety of strategies incorporating various types of adsorbates, such as electric field-responsive adsorbates,[11,12] light-active adsorbates,[13,14] ion-exchangeable adsorbates,[15] and mixtures of adsorbates.[16,20−23] The approach taken by Lahann and co-workers was to prepare loosely packed carboxylate-terminated alkanethiolate SAMs on gold surfaces.[11] These films responded to a change in the electrical potential of the substrate: the hydrophilic carboxylate groups initially at the interface were drawn to the substrate, leaving loops of the hydrophobic alkyl chains at the interface. Chen and co-workers designed and synthesized UV light-active thiol adsorbates to modulate the interfacial wettability of gold

Received: April 7, 2016
Revised: July 5, 2016
Published: July 7, 2016

DOI: 10.1021/acs.chemmater.6b01390
Chem. Mater. 2016, 28, 5356−5364

surfaces.[13] The conformation of the terminal perfluoro moiety was transformed by exposure to UV light (365 nm), thereby burying it in the film and changing the surface wettability. Chi and co-workers manipulated the wettability of imidazolium-terminated surfaces by exchanging counteranions.[15] The contact angles for water on PF_6^- anion-modified surfaces were markedly higher than those on Cl^- anion-modified surfaces.

One of the limitations of the aforementioned three strategies is that they require external stimuli to control the surface wettability. However, Portilla and Halik easily tailored the surface wettability of aluminum oxide by changing the ratio of perfluoro-terminated phosphonic acid to oligo(ethylene glycol)-terminated phosphonic acid in the SAM development solutions.[16] While this method also appears applicable for controlling the wettability of gold surfaces using mixtures of alkanethiols instead of alkyl phosphonic acids, three critical problems exist: (1) The solution composition and surface composition often vary. (2) The composition of the adsorbates on the surfaces changes with time. (3) Macroscopic/microscopic phase-separation of the adsorbates can occur.[24−26] These phenomena limit control over the interfacial wettability of mixed SAMs generated from monothiol adsorbates and are due in large part to the nature of the bonding between the adsorbates and substrate. Phosphonic acid adsorbates are not subject to the surface migration experienced by monothiols on noble metals because of the multiple surface interactions between the phosphonic acid headgroups and the substrate. However, typical alkanethiol adsorbates on gold not only relocate on these surfaces, but are also easily exchanged with adsorbates in the development solution because of the labile S−Au bonds. For example, Whitesides and co-workers investigated the wettability and structural properties of mixed SAMs derived from mixtures of CH_3-terminated alkanethiols and $HOCH_2$-terminated alkanthiols,[23,24,27] finding that long methylene linkers enhanced the stability of mixed SAMs. However, these monodentate adsorbates failed to show the linear wettability trends over all compositions. In an effort to overcome the disadvantages of monodenate alkanethiols for the generation of mixed SAMs, Schönherr and co-worker utilized alkyl fluoroalkyl disulfides to generate mixed SAMs.[28,29] The mixed SAMs were formed by coadsorption from solutions containing equal amounts of the corresponding disulfides. However, unsymmetrical disulfides, given their fixed 1:1 ratio of terminal groups and their potential for cleavage on the surface and subsequent desorption, are unsuitable candidates for precisely controlling surface wettability.

With these considerations in mind, we designed and synthesized a set of new perfluoro-, *n*-alkyl-, and oligo(ethylene glycol)-terminated adsorbates in an effort toward the generation of highly stable mixed monolayers to enhance the control of interfacial wettability. The new custom-designed adsorbates are (5-(9,9,10,10,11,11,12,12,13,13,14,14,15,15,16,16,16-heptadecafluorohexadecyloxy)-1,3-phenylene)dimethanethiol (**PFPDT**), (5-(hexadecyloxy)-1,3-phenylene)dimethanethiol (**HDPDT**), and (5-(2,5,8,11-tetraoxahexadecan-16-yloxy)-1,3-phenylene)-dimethanethiol (**OEGPDT**) (see Figure 1). The key structural feature of these adsorbates consists of a dithiol headgroup for enhancing the stability of the resulting SAMs, as demonstrated in previous studies.[30−32] The bidentate adsorbates bind strongly to the surface of gold and therefore resist desorption and exchange with adsorbates in solution.[30] To provide a more complete analysis of the effectiveness of this new class of multidentate adsorbate, we prepared a control system of analogous monothiol adsorbates having pefluoro-, *n*-alkyl-, and oligo(ethylene glycol)-terminal groups, and these are 9,9,10,10,11,11,12,12,13,13,14,14,15,15,16,16,16-heptadecafluorohexadecane-1-thiol (**PFT**), hexadecane-1-thiol (**HDT**), and 2,5,8,11-tetraoxahexadecane-16-thiol (**OEGT**) (see Figure 1).

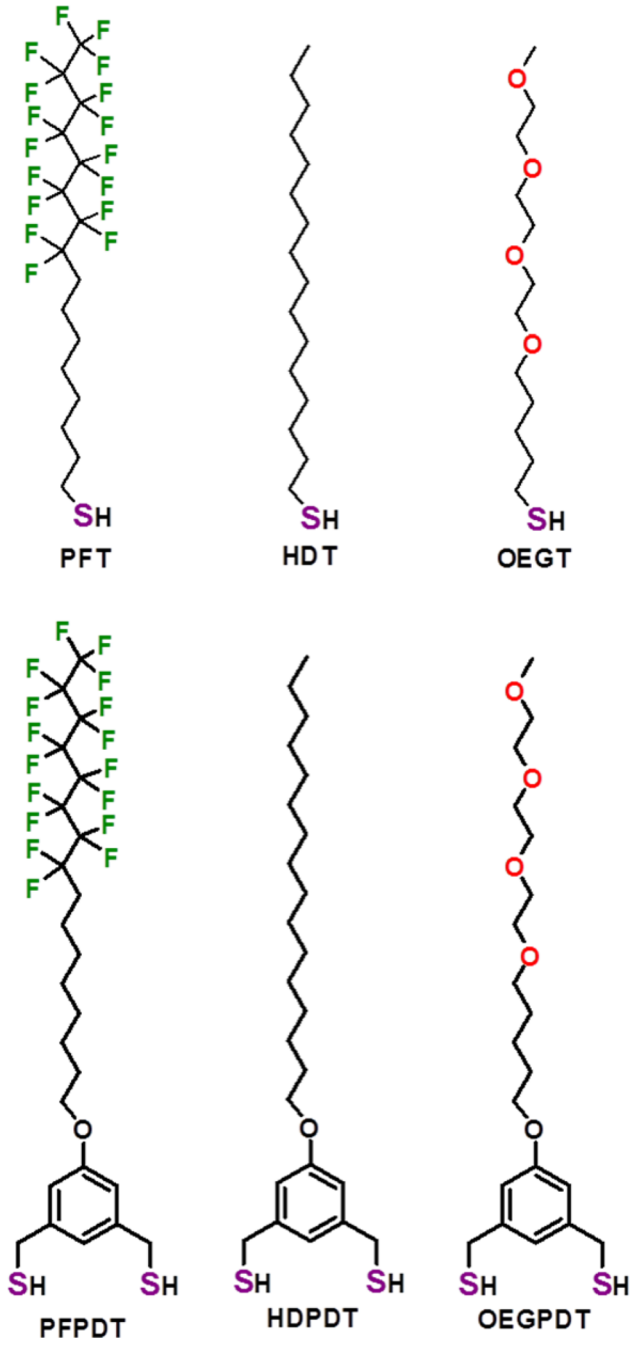

Figure 1. Illustration of the structures of the monodentate and bidentate perfluoro-, *n*-alkyl-, and oligo(ethylene glycol)-terminated alkanethiols.

Herein, we explore judicious sets of mixed SAMs prepared from the six adsorbates shown in Figure 1: the first set of mixed SAMs was generated exclusively from the monodentate adsorbates (**PFT**, **HDT**, and **OEGT**), while the second set of mixed SAMs was generated exclusively from the bidentate

DOI: 10.1021/acs.chemmater.6b01390
Chem. Mater. 2016, 28, 5356−5364

Table 1. Mole Fractions of Adsorbates in Ethanolic Solution Used to Develop the Mixed SAMs

	mole fraction of monodentate adsorbate in the development solution[a]				mole fraction of bidentate adsorbate in the development solution[a]		
SAM abbreviation	**PFT**	**HDT**	**OEGT**	SAM abbreviation	**PFPDT**	**HDPDT**	**OEGPDT**
PFT (1.00)	1.00	0.00	0.00	**PFPDT (1.00)**	1.00	0.00	0.00
PFT (0.75)	0.75	0.25	0.00	**PFPDT (0.75)**	0.75	0.25	0.00
PFT (0.50)	0.50	0.50	0.00	**PFPDT (0.50)**	0.50	0.50	0.00
PFT (0.25)	0.25	0.75	0.00	**PFPDT (0.25)**	0.25	0.75	0.00
HDT	0.00	1.00	0.00	**HDPDT**	0.00	1.00	0.00
OEGT (0.25)	0.00	0.75	0.25	**OEGPDT (0.25)**	0.00	0.75	0.25
OEGT (0.50)	0.00	0.50	0.50	**OEGPDT (0.50)**	0.00	0.50	0.50
OEGT (0.75)	0.00	0.25	0.75	**OEGPDT (0.75)**	0.00	0.25	0.75
OEGT (1.00)	0.00	0.00	1.00	**OEGPDT (1.00)**	0.00	0.00	1.00

[a]The overall thiol concentration was maintained at 1.0 mM.

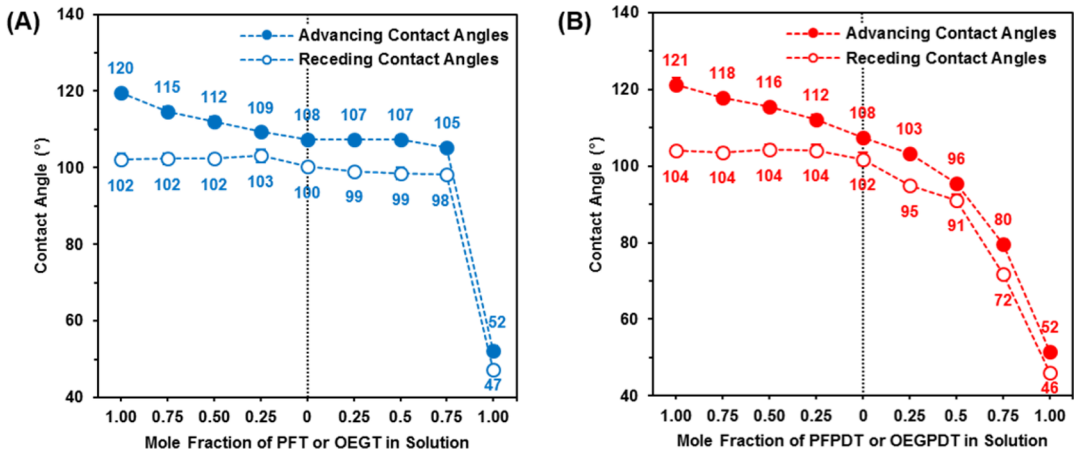

Figure 2. Advancing and receding contact angles of water on the mixed SAM series derived from (A) the monodentate alkanethiols (**PFT**, **HDT**, and **OEGT**) and (B) the bidentate alkanethiols (**PFPDT**, **HDPDT**, and **OEGPDT**) in ethanol. For each series, contact angles for the single-component *n*-alkyl-terminated SAM is the mole fraction 0 in the plot. Error bars that are not visible fall within the symbols.

adsorbates (**PFPDT**, **HDPDT**, and **OEGPDT**). There are large differences in hydrophilicity/hydrophobicity and solubility between the PF-terminated and the OEG-terminated adsorbates. Therefore, we prepared mixed SAMs generated from binary mixtures of hydrocarbon adsorbates (**HDPDT** and **HDT**) blended with PF adsorbates (**PFPDT** and **PFT**) and separately with OEG adsorbates (**OEGPDT** and **OEGT**) in this study. Future studies will examine more complicated systems, such as PF + OEG and ternary mixtures of HC, PF, and OEG. The wettability of all of the mixed SAMs was evaluated by contact angle goniometry using water as a contacting liquid. Qualitative and quantitative analyses of the SAMs were conducted by ellipsometry, X-ray photoelectron spectroscopy (XPS), and polarization modulation infrared reflection−absorption spectroscopy (PM-IRRAS). Furthermore, a stability study was conducted to evaluate the potential of these SAMs as coating materials for controlling surface wettability.

EXPERIMENTAL SECTION

Details regarding the materials, procedures, and instrumentation used to conduct the research reported in this manuscript are provided in the Supporting Information, including ^{1}H and ^{13}C NMR spectra for all new perfluoro-, *n*-alkyl-, and oligo(ethylene glycol)-terminated alkanedithiols (see Figures S1−S6).

RESULTS AND DISCUSSION

Allara and co-workers reported that the composition of adsorbates on gold was constant after incubation for 12 h; however, these researchers characterized mixed SAMs developed for 48 h to ensure that the mixed SAMs reached complete equilibrium states.[33] We have followed this protocol in the work reported here. Accordingly, evaporated gold slides were immersed in ethanolic solutions containing the mixture of thiols for 48 h at room temperature. Deposition solutions were prepared with the various ratios of adsorbates shown in Table 1, with the overall thiol concentration maintained at 1.0 mM. To provide a simplified means of identifying specific SAMs in our two series of mixed-adsorbate films, a set of abbreviations are also provided in Table 1.

A. Wettability. The hydrophobicity and hydrophilicity of the films generated from mixtures of the perfluoro-, *n*-alkyl-, and oligo(ethylene glycol)-terminated adsorbates were evaluated by obtaining the advancing (θ_a) and receding (θ_r) contact angles for water. Figure 2A provides the profile of the θ_a and θ_r values for water on the SAMs generated from the mixtures of the monodentate adsorbates (**PFT**, **HDT**, and **OEGT**). Values of θ_a measured on the single-component **PFT**, **HDT**, and **OEGT** films were 120, 108, and 52°, respectively. The difference in the θ_a values for **PFT (1.00)** and **HDT** was 12°, and the θ_a on the films of the mixed SAM series generated from **PFT** and **HDT** gradually decreased with a decrease in the fraction of **PFT** in the development solutions. For the mixed

DOI: 10.1021/acs.chemmater.6b01390
Chem. Mater. 2016, 28, 5356−5364

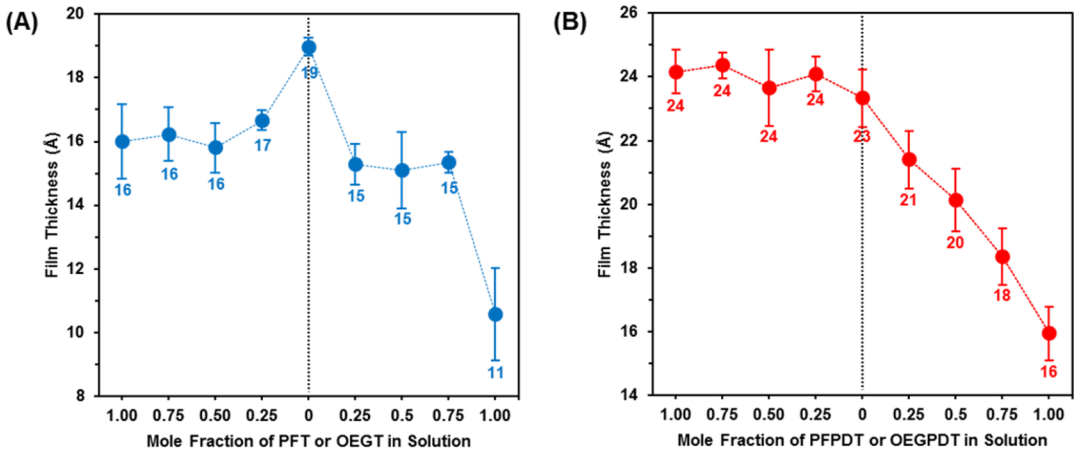

Figure 3. Ellipsometric film thicknesses for the mixed SAM series derived from (A) the monodentate alkanethiols (**PFT**, **HDT**, and **OEGT**) and (B) the bidentate alkanethiols (**PFPDT**, **HDPDT**, and **OEGPDT**) in ethanol. For each series, θ_a for the single-component *n*-alkyl-terminated SAM is the mole fraction 0 in the plot. Error bars indicate the standard deviation for the data.

SAMs, each of the data points fall below a line directly connecting the two single-component SAMs, which might indicate a deficit of the **PFT** adsorbate in these SAMs. The difference in θ_a values between **HDT** and **OEGT** (**1.00**) was 56°, which was much larger than that between **PFT** (**1.00**) and **HDT**; nevertheless, the θ_a's on the films of the mixed SAM series generated from **HDT** and **OEGT** were nearly constant, with the θ_a for the **OEGT** SAM reflecting a dramatic change in wettability. Interestingly, while the single-component bidentate SAMs (**PFPDT**, **HDPDT**, and **OEGPDT**) produced essentially the same results as the analogous single-component monodentate SAMs (121, 108, and 52°, respectively), a different set of trends was observed for θ_a for the films generated from the *mixtures* of bidentate adsorbates (Figure 2B). A decrement in the θ_a values was observed in the range of **PFPDT** (**1.00**) to **HDPDT**, results in common with the trend for the θ_a values on the mixed SAMs generated from the mixture of **PFT** and **HDT**. The difference in the advancing contact angle values for water between **PFPDT** (**1.00**) and **HDPDT** (13°) was similar to that between **PFT** (**1.00**) and **HDT** (12°); yet for the associated mixed SAMs, each of the data points lie slightly above a line directly connecting the two single-component SAMs. Additionally, θ_a for water on the **HDPDT**/**OEGPDT**-mixed SAMs gradually decreased with an increase in the fraction of **OEGPDT** in the development solutions. We also plotted the advancing (θ_a) and receding (θ_r) contact angles as a function of cos(θ) to evaluate the changes in surface energy (see Figure S7 in the Supporting Information). The trends in the cosine values follow those of contact angles. Therefore, these results illustrate the advantages of the bidentate adsorbates to control the surface energy as well as the wettability. Furthermore, we calculated the hystereses ($\theta_a - \theta_r$) for all of the SAMs (see Table S1 in the Supporting Information); notably, these measurements showed that the hysteresis data for the series of mixed bidentate SAMs closely align with those of the analogous films in the series of mixed monodentate SAMs. These results suggest that the bidentate adsorbates form generally well-ordered films with comparable interfacial chain packing to that of the monothiolate monolayers on gold surfaces. In further efforts to determine the origin of the differing trends in wettability between the series of monodentate mixed SAMs and that of the bidentate mixed SAMs, we analyzed these films by ellipsometry, XPS, and PM-IRRAS, as described below.

B. Ellipsometric Thickness. The thicknesses of the films for both mixed SAM series were measured using ellipsometry. The average values for the collected data are plotted in Figure 3. The ellipsometric thicknesses of the films generated from **PFT** (**1.00**), **HDT**, and **OEGT** (**1.00**) in ethanol correspond well with reference values obtained from the literature (see Figure 3A).[34−36] Even though **PFT**, **HDT**, and **OEGT** have similar molecular lengths (the total number of carbons and oxygens in chains of adsorbates is 16), the thicknesses of the SAMs derived from these adsorbates were influenced by the nature of the backbone. While **HDT** forms well-ordered and densely packed SAMs (film thickness = 19 Å), the bulky perfluorinated backbone of **PFT** and the flexible oligoethylene glycol backbone of **OEGT** give rise to SAMs with lesser chain packing densities and consequently lesser ellipsometric thicknesses (16 and 11 Å, respectively). We expected the film thickness values of the mixed SAMs to lie between those of the pure single-component SAMs and to gradually increase (or decrease) between these two values. However, the thicknesses of the SAMs generated from the mixture of two monodentate adsorbates were nearly constant: ∼16−17 Å for the **PFT**/**HDT**-mixed SAMs and ∼15 Å for the **HDT**/**OEGT**-mixed SAMs, even though the single-component SAMs for **PFT** (**1.00**), **HDT**, and **OEGT** (**1.00**) were 16, 19, and 11 Å, respectively. In contrast, the ellipsometric thickness measurements of all of the SAMs derived from **PFPDT** and **HDPDT** showed films that exhibited statistically equivalent thicknesses (see Figure 3B). Furthermore, the thicknesses of the **OEGPDT**/**HDPDT**-mixed SAMs gradually decreased with an increase in the fraction of **OEGPDT** in the development solutions, yielding a linear trend for the thickness data for the second half of this mixed SAM series (see Figure 3B).

C. Analysis by XPS. XPS is a useful tool for the qualitative and quantitative analysis of SAMs, including the characterization of the surface bonds, determination of the atomic composition, and estimation of the surface density of the adsorbates. In the present study, we examined the surface composition of the adsorbates in the mixed SAMs by analyzing the X-ray photoelectron spectra of the C 1s region. The C 1s peaks of the perfluorocarbon moieties appear at ∼291 eV and ∼293 eV.[37,38] The peaks at ∼286.6 eV indicate the presence of

DOI: 10.1021/acs.chemmater.6b01390
Chem. Mater. 2016, 28, 5356−5364

the etheric carbons of the ethylene glycol chains,[39,40] and the peaks at ~285 eV are characteristic of saturated hydrocarbons.[31,32] For the monodentate adsorbates, the intensity of the peaks associated with the perfluorocarbon moieties (binding energies = ~291 eV and ~293 eV) in the **PFT**/**HDT**-mixed SAMs decreased with the decrease in the fraction of **PFT** in the development solutions (see Figure 4A).

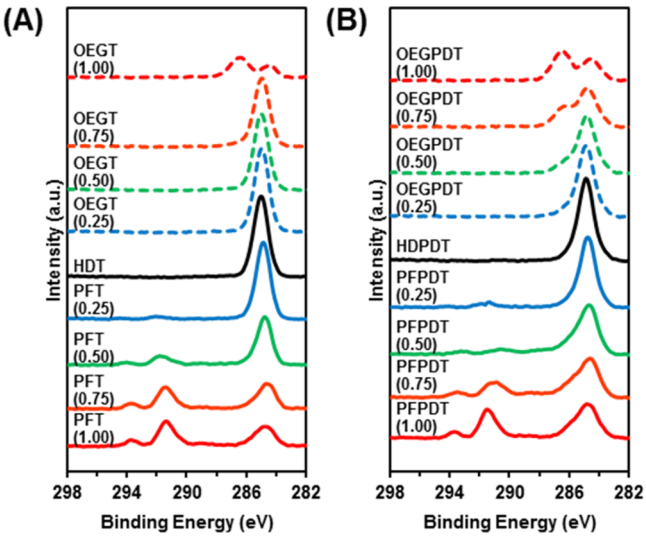

Figure 4. X-ray photoelectron spectra of the C 1s region of the mixed SAM series derived from (A) the monodentate alkanethiols (**PFT**, **OEGT**, and **HDT**) and (B) the bidentate alkanethiols (**PFPDT**, **HDPDT**, and **OEGPDT**) in ethanol.

However, the peak for the ethylene glycol carbons (binding energy = ~286.6 eV) was not observed in the monodentate **HDT**/**OEGT**-mixed SAMs (**OEGT (0.25)**, **OEGT (0.50)**, and **OEGT (0.75)**). For the bidentate adsorbates, both the decrements in the intensity of the peaks associated with the perfluorocarbon moieties and the increments in the intensity of the peaks associated with the ethylene glycol carbons varied systematically with the changes in the adsorbate ratios of the development solutions for the mixed SAMs generated from the bidentate adsorbates (**PFPDT**/**HDPDT** and **HDPDT**/**OEGPDT**) (see Figure 4B). These results indicate that the perfluoro-terminated alkanethiols (**PFT** and **PFPDT**) and the *n*-alkyl-terminated alkanethiols (**HDT** and **HDPDT**) form mixed SAMs that vary with the ratios of their ethanolic development solutions on gold surfaces, even with the differences in the thiol headgroups. In contrast, for the oligo(ethylene glycol)-terminated alkanedithiols (**OEGT** and **OEGDT**), only the SAMs formed from the bidentate alkanethiol mixture (**HDPDT** and **OEGDT**) generated XPS data that would indicate that they form *n*-alkyl- and oligo(ethylene glycol)-terminated mixed SAMs that align with the composition of their ethanolic development solutions.

For a quantitative analysis of the changes in the composition ratios of the adsorbates in the two series of mixed SAMs, fluorine-to-carbon (F/C) and oxygen-to-carbon (O/C) ratios were calculated from the integrated peak areas associated with the spectral data of the F 1s, O 1s, and C 1s regions from the X-ray photoelectron spectra. The F/C ratios for the number of elements in adsorbates are different (**PFT**: 17 fluorines/16 carbons = 1.06; **PFPDT**: 17 fluorines/24 carbons = 0.71). Therefore, the F/C ratios of XPS intensities the pure 1.00 **PFT** SAM (4.71) and the pure 1.00 **PFPDT** SAM (3.56) are different. However, the F/C ratios of the films for both series of mixed SAMs formed from combinations of **PFT**/**HDT** and **PFPDT**/**HDPDT** exhibit an almost linear decrease with a decrease in the fraction of **PFT** and **PFPDT** in the development solutions, respectively (see Figure 5, plots A1 and A2), with this trend being much more clearly defined for the SAMs formed from the bidentate adsorbates. In contrast with the trends of the F/C ratios, substantially different trends were observed in the O/C ratios between the two series of mixed SAMs. The O/C ratios of the SAMs generated from mixtures of the monodentate adsorbates **HDT** and **OEGT** remained at or near zero until the fraction of **OEGT** in solution was increased to 0.75 (see Figure 5, plot B1). In contrast, the O/C ratios of the **HDPDT**/**OEGPDT**-mixed SAMs on gold surfaces gradually increased with an increase in the fraction of **OEGPDT** in the development solutions (see Figure 5, plot B2). For plot B2, the attenuated signal from the oxygen atom on the phenyl ring produces a minor increase in the O/C ratio for all of the **HDPDT**/**OEGPDT**-mixed SAMs.

The quantitative analysis of the elemental content of the films is consistent with the qualitative analysis of the C 1s X-ray photoelectron spectra of both series of mixed SAMs described in the preceding paragraph.

The change in advancing contact angles (θ_a) of water on the mixed SAM series as a function of the fluorine-to-carbon (F/C) ratios and the oxygen-to-carbon (O/C) ratios for the SAMs was evaluated by quantitative analysis of X-ray photoelectron spectra and contact angle data (see Figure S8 in the Supporting Information). Interestingly, the slope of the trend lines for the bidentate mixed SAMs (Figure S8, plots A2 and B2) is 50% steeper than that for the monodentate-mixed SAMs (Figure S8, plots A1 and B1). These results indicate that the bidentate adsorbates are superior to the monodentate adsorbates for providing precise control of the interfacial wettability.

D. Analysis by PM-IRRAS. Surface infrared spectroscopy can provide additional insight into the composition and conformational order of SAMs. The degree of conformational order of the alkyl chains in the SAMs can be estimated by the peak position of the methylene antisymmetric C−H stretching vibration ($\nu_a^{CH_2}$) obtained using polarization modulation infrared reflection−absorption spectroscopy (PM-IRRAS).[41−44] For example, $\nu_a^{CH_2}$ for a highly ordered heptadecanethiolate SAM is ~2919 cm^{-1}; however, that of the corresponding disordered SAM after partial thermal desorption was ~2924 cm^{-1}.[44] Two noteworthy observations can be made with regard to the PM-IRRAS spectral data in Figure 6. First, the band positions of the antisymmetric methylene C−H stretching vibration ($\nu_a^{CH_2}$) for the mixed SAMs generated from the monodentate adsorbates (**PFT**, **HDT**, and **OEGT**) are nearly constant (2919−2920 cm^{-1}) throughout the series, and those for the mixed SAMs generated from the bidentate adsorbates (**PFPDT**, **HDPDT**, and **OEGPDT**) are also nearly constant, but at higher wavenumbers (2924−2925 cm^{-1}). These results indicate that the degree of conformational order of the alkyl chains in the mixed SAMs generated from the monodentate adsorbates is greater than that in the mixed SAMs generated from the bidentate adsorbates.[41,45] However, the conformational order of the alkyl chains in the series of mixed SAMs generated from the same form of headgroup (monodentate versus bidentate) produced almost the same $\nu_a^{CH_2}$ peak positions, regardless of the ratio of the adsorbates in the development solution. Second, the methyl

DOI: 10.1021/acs.chemmater.6b01390
Chem. Mater. 2016, 28, 5356−5364

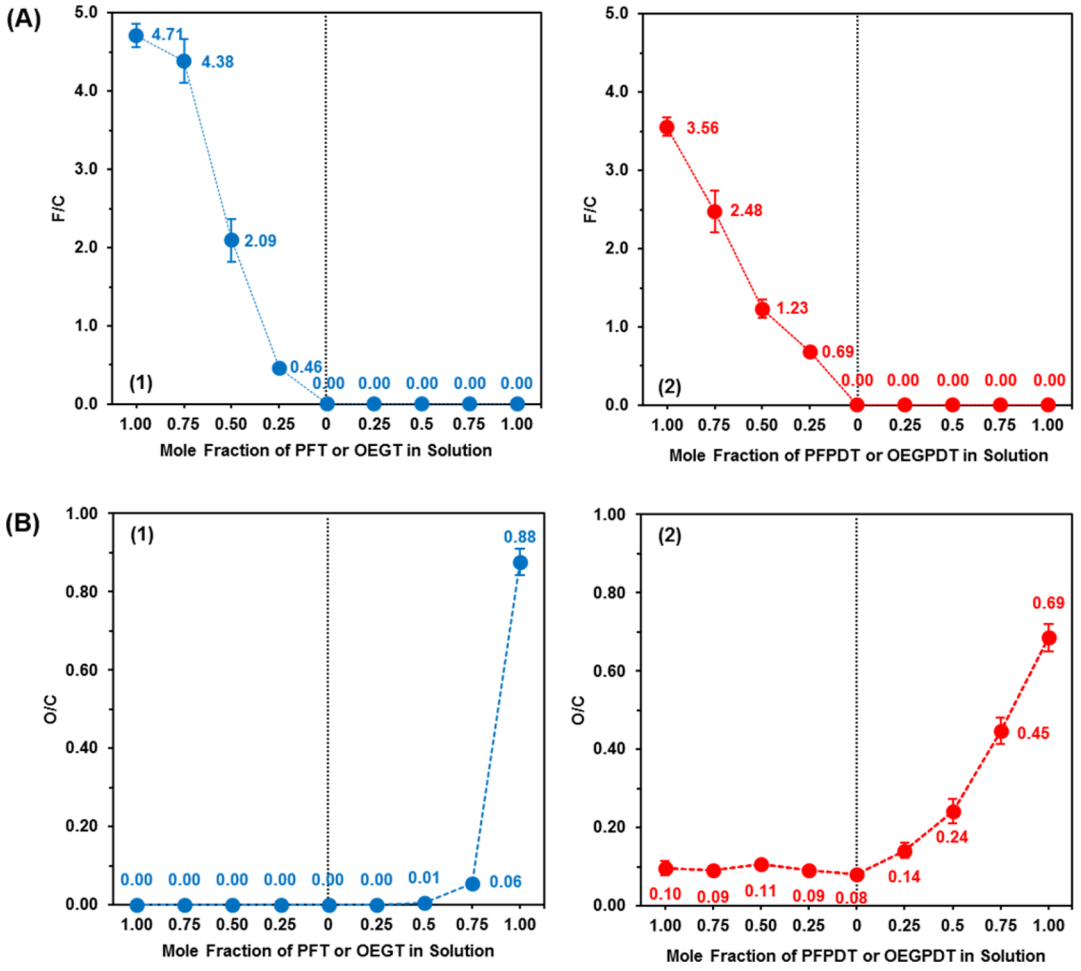

Figure 5. XPS-derived elemental data for both series of mixed SAMs for (A) the fluorine-to-carbon (F/C) ratios and (B) the oxygen-to-carbon (O/C) ratios for the SAMs derived from (1) the monodentate alkanethiols (**PFT**, **HDT**, and **OEGT**) and (2) the bidentate alkanethiols (**PFPDT**, **HDPDT**, and **OEGPDT**) in ethanol. Error bars indicate the standard deviation for the data. Error bars that are not visible fall within the symbols.

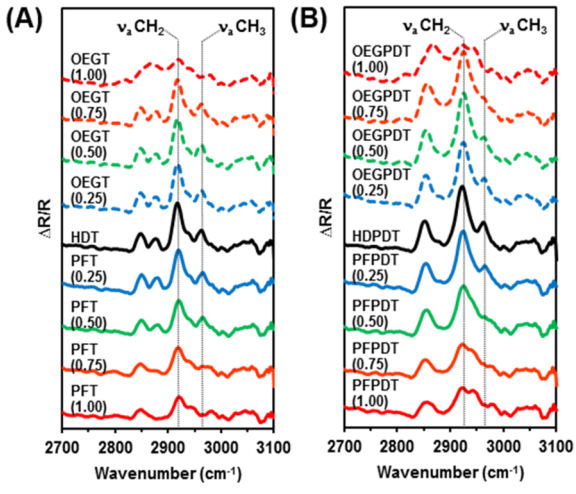

Figure 6. PM-IRRAS spectra of the SAMs derived from (A) the monodentate alkanethiols (**PFT**, **HDT**, and **OEGT**) and (B) the bidentate alkanethiols (**PFPDT**, **HDPDT**, and **OEGPDT**) in ethanol.

antisymmetric C−H stretching vibration ($\nu_a^{CH_3}$ = ∼2965 cm^{-1})[41] for the series of mixed SAMs generated from the monodentate adsorbates (**PFT**, **HDT**, and **OEGT**) are detectable in the spectra for the series over the range of **PFT** (**0.50**) to **OEGT** (**0.75**) and exhibit similar peak intensities. These results align well with the XPS data presented in Figure 5. Interestingly, $\nu_a^{CH_3}$ for the mixed SAMs generated from the bidentate adsorbates (**PFPDT**, **HDPDT**, and **OEGPDT**) are detectable in the spectra over the range of **PFPDT** (**0.50**) to **OEGPDT** (**0.50**) and exhibit a steady loss of peak intensity with an increase in the fraction of **PFPDT** or **OEGPDT** in the development solution. These data are consistent with those obtained by the instrumental methods described above inasmuch as the intensity of the $\nu_a^{CH_3}$ bands reflect the presence of the *n*-alkyl-terminated adsorbates in the mixed SAMs.

E. Evaluation of Stability. Solution-phase displacement tests were conducted to evaluate the stability of the adsorbates in each series of mixed SAMs. To perform these experiments, fully developed mixed SAM slides were immersed in 10 mM ethanolic solutions containing *n*-alkanethiols (**HDT** or **HDPDT**) for 48 h at room temperature: **HDT** and **HDPDT** were used as the displacing agents for the monodentate mixed SAMs and the bidentate mixed SAMs, respectively. Figure 7 demonstrates the remarkable difference in stability between the monodentate and bidentate films. Before the displacement tests for the series of mixed SAMs formed from **PFT**, **HDT**, and **OEGT**, the advancing contact angles (θ_a) of water on the mixed SAMs generated from **PFT** and **HDT** exhibited a gradual but steady decrease in the θ_a values, while those for **HDT** and **OEGT** showed little change (∼107°) except for the θ_a value on

DOI: 10.1021/acs.chemmater.6b01390
Chem. Mater. 2016, 28, 5356−5364

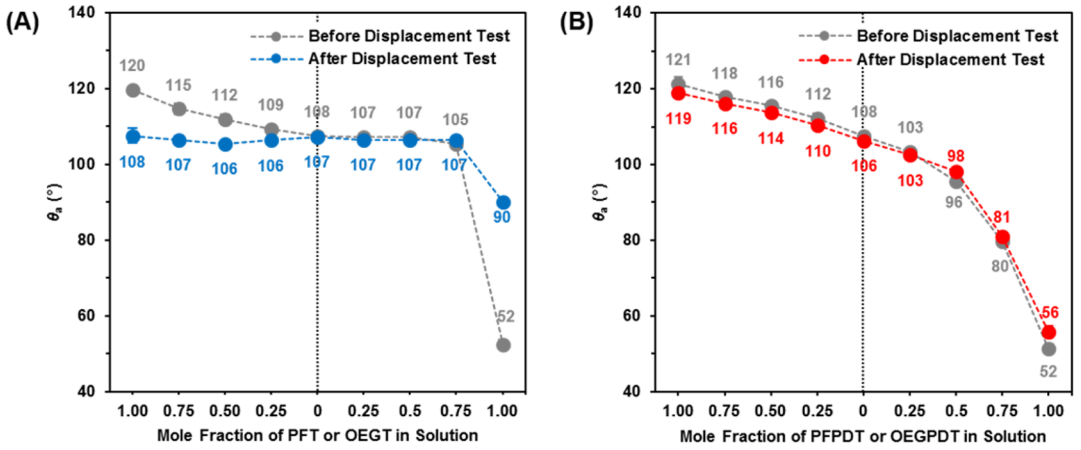

Figure 7. Advancing contact angles (θ_a) of water on the series of mixed SAMs derived from (A) the monodentate alkanethiols (**PFT**, **HDT**, and **OEGT**) and (B) the bidentate alkanethiols (**PFPDT**, **HDPDT**, and **OEGPDT**) before and after a second immersion in an ethanolic solution containing only **HDT** (10 mM) for monodentate-mixed SAMs and only **HDPDT** (10 mM) for bidentate-mixed SAMs for 48 h at rt. Error bars that are not visible fall within the symbols.

the pure **OEGT** SAM, which dropped to 52°. However, the θ_a values measured for the series of mixed SAMs after performing the displacement tests were nearly constant (~107°) except that the θ_a value on the pure **OEGT** SAM increased from 52° to 90° in the 10 mM ethanolic solution of **HDT** (see Figure 7A). Interestingly, θ_a's on the series of mixed SAMs generated from the bidentate adsorbates (**PFPDT**, **HDPDT**, and **OEGPDT**) retained their general trend of a gradual decrease in the advancing contact angles from the most hydrophobic surface generated from 100% of **PFPDT** to the most hydrophilic surface generated from 100% of **OEGPDT** (Figure 7B). These experimental results indicate that **PFT** and **OEGT** on the gold surfaces were mostly replaced by the **HDT** adsorbates during the 48 h of exposure to the adsorbate solution, but **PFPDT** and **OEGPDT** had a markedly greater propensity to remain on the gold surfaces during the displacement tests. These experimental results thus provide further evidence that the entropy-driven chelate effect associated with the bidentate headgroup plays an important role in enhancing the stability of SAMs formed from bidentate adsorbates.[46] More specifically, upon introduction to the surface of gold, the bidentate adsorbates bind strongly with little or no reversible desorption, even in solutions containing displacing adsorbates at high concentration. Therefore, the surface composition of the bidentate adsorbates depends largely on the initial composition of the deposition solution. In contrast, the monodentate adsorbates readily undergo desorption and exchange with adsorbates in solution.[25] Therefore, the composition of the monodentate mixed SAMs on the surfaces readily undergo changes when displacing adsorbates are present in solution.

CONCLUSIONS

Mixtures of perfluoro-, *n*-alkyl-, and oligo(ethylene glycol)-terminated alkanethiols and alkanedithiols were utilized for controlling the wettability of SAMs on gold surfaces. The hydrophobicity and hydrophilicity of the mixed SAMs formed from the bidentate adsorbates were readily tuned by the fraction of **PFPDT** or **OEGPDT** in the development solutions. However, the interfacial properties of the mixed SAMs formed from the monodentate adsorbates failed to correlate directly with the fraction of **PFT** or **OEGT** in their development solutions. More specifically, analysis of the mixed monolayers by ellipsometry, XPS, and PM-IRRAS revealed that the bidentate adsorbates (**PFPDT**, **HDPDT**, and **OEGPDT**) readily formed mixed monolayers with composition ratios of **PFPDT**/**HDPDT** and **HDPDT**/**OEGPDT** that closely aligned with that of their development solutions; in contrast, the composition ratios of the monodentate adsorbates (**PFT**, **HDT**, and **OEGT**) in their mixed SAMs failed to align with the composition of their development solutions. Furthermore, the series of mixed monolayer films derived from the bidentate adsorbates showed remarkable stability during solution-phase displacement tests. We conclude that the unique and valuable behavior of the mixed SAMs generated from the bidentate adsorbates arises from the entropy-driven chelate effect. Overall, mixed monolayers derived from perfluoro-, *n*-alkyl-, and oligo(ethylene glycol)-terminated bidentate thiols offer a uniquely convenient and reliable method to control the wettability of surfaces.

ASSOCIATED CONTENT

Supporting Information

The Supporting Information is available free of charge on the ACS Publications website at DOI: 10.1021/acs.chemmater.6b01390.

Detailed descriptions of the materials and synthetic procedures for preparing the perfluoro-, *n*-alkyl-, and oligo(ethylene glycol)-terminated alkanedithiols, along with the instrumental procedures used to conduct this research and additional contact angle data (PDF)

AUTHOR INFORMATION

Corresponding Author

*E-mail: trlee@uh.edu.

Notes

The authors declare no competing financial interest.

ACKNOWLEDGMENTS

We thank the National Science Foundation (CHE-1411265), the Robert A. Welch Foundation (grant no. E-1320), and the Texas Center for Superconductivity at the University of Houston for generous support.

DOI: 10.1021/acs.chemmater.6b01390
Chem. Mater. 2016, 28, 5356−5364

REFERENCES

(1) Sun, T.; Wang, G.; Liu, H.; Feng, L.; Jiang, L.; Zhu, D. Control over the Wettability of an Aligned Carbon Nanotube Film. *J. Am. Chem. Soc.* **2003**, *125*, 14996−14997.

(2) Zheng, Z.; Azzaroni, O.; Zhou, F.; Huck, W. T. S. Topography Printing to Locally Control Wettability. *J. Am. Chem. Soc.* **2006**, *128*, 7730−7731.

(3) Kawai, T.; Suzuki, M.; Kondo, T. Fabrication of Flexible Gold Films with Periodic Sub-Micrometer Roughness and Their Wettability Control by Modification of SAM. *Langmuir* **2006**, *22*, 9957−9961.

(4) Fukuzawa, K.; Deguchi, T.; Yamawaki, Y.; Itoh, S.; Muramatsu, T.; Zhang, H. Control of Wettability of Molecularly Thin Liquid Films by Nanostructures. *Langmuir* **2008**, *24*, 2921−2928.

(5) Lee, M.; Kwak, G.; Yong, K. Wettability Control of ZnO Nanoparticles for Universal Applications. *ACS Appl. Mater. Interfaces* **2011**, *3*, 3350−3356.

(6) Lee, M. W.; An, S.; Joshi, B.; Latthe, S. S.; Yoon, S. S. Highly Efficient Wettability Control via Three-Dimensional (3D) Suspension of Titania Nanoparticles in Polystyrene Nanofibers. *ACS Appl. Mater. Interfaces* **2013**, *5*, 1232−1239.

(7) Pakdel, A.; Bando, Y.; Golberg, D. Plasma-Assisted Interface Engineering of Boron Nitride Nanostructure Films. *ACS Nano* **2014**, *8*, 10631−10639.

(8) Li, L.; Zhu, Y.; Li, B.; Gao, C. Fabrication of Thermoresponsive Polymer Gradients for Study of Cell Adhesion and Detachment. *Langmuir* **2008**, *24*, 13632−13639.

(9) Pei, Y.; Travas-Sejdic, J.; Williams, D. E. Reversible Electrochemical Switching of Polymer Brushes Grafted onto Conducting Polymer Films. *Langmuir* **2012**, *28*, 8072−8083.

(10) Nguyen, P. Q. M.; Yeo, L.-P.; Lok, B.-K.; Lam, Y.-C. Patterned Surface with Controllable Wettability for Inkjet Printing of Flexible Printed Electronics. *ACS Appl. Mater. Interfaces* **2014**, *6*, 4011−4016.

(11) Lahann, J.; Mitragotri, S.; Tran, T.-N.; Kaido, H.; Sundaram, J.; Choi, I. S.; Hoffer, S.; Somorjai, G. A.; Langer, R. A Reversibly Switching Surface. *Science* **2003**, *299*, 371−374.

(12) Pei, Y.; Ma, J. Electric Field Induced Switching Behaviors of Monolayer-Modified Silicon Surfaces: Surface Designs and Molecular Dynamics Simulations. *J. Am. Chem. Soc.* **2005**, *127*, 6802−6813.

(13) Chen, K.-Y.; Ivashenko, O.; Carroll, G. T.; Robertus, J.; Kistemaker, J. C. M.; London, G.; Browne, W. R.; Rudolf, P.; Feringa, B. L. Control of Surface Wettability Using Tripodal Light-Activated Molecular Motors. *J. Am. Chem. Soc.* **2014**, *136*, 3219−3224.

(14) Kwak, G.; Lee, M.; Senthil, K.; Yong, K. Wettability Control and Water Droplet Dynamics on SiC-SiO_2 Core-Shell Nanowires. *Langmuir* **2010**, *26*, 12273−12277.

(15) Chi, Y. S.; Lee, J. K.; Lee, S.; Choi, I. S. Control of Wettability by Anion Exchange on Si/SiO_2 Surfaces. *Langmuir* **2004**, *20*, 3024−3027.

(16) Portilla, L.; Halik, M. Smoothly Tunable Surface Properties of Aluminum Oxide Core-Shell Nanoparticles by A Mixed-Ligand Approach. *ACS Appl. Mater. Interfaces* **2014**, *6*, 5977−5982.

(17) Ulman, A. Formation and Structure of Self-Assembled Monolayers. *Chem. Rev.* **1996**, *96*, 1533−1554.

(18) Love, J. C.; Estroff, L. A.; Kriebel, J. K.; Nuzzo, R. G.; Whitesides, G. M. Self-Assembled Monolayers of Thiolates on Metals as a Form of Nanotechnology. *Chem. Rev.* **2005**, *105*, 1103−1169.

(19) Vericat, C.; Vela, M. E.; Benitez, G.; Carro, P.; Salvarezza, R. C. Self-Assembled Monolayers of Thiols and Dithiols on Gold: New Challenges for a Well-Known System. *Chem. Soc. Rev.* **2010**, *39*, 1805−1834.

(20) Bain, C. D.; Whitesides, G. M. Molecular-Level Control over Surface Order in Self-Assembled Monolayer Films of Thiols on Gold. *Science* **1988**, *240*, 62−63.

(21) Bain, C. D.; Evall, J.; Whitesides, G. M. Formation of Monolayers by the Coadsorption of Thiols on Gold: Variation in the Head Group, Tail Group, and Solvent. *J. Am. Chem. Soc.* **1989**, *111*, 7155−7164.

(22) Bain, C. D.; Whitesides, G. M. Formation of Monolayers by the Coadsorption of Thiols on Gold: Variation in the Length of the Alkyl Chain. *J. Am. Chem. Soc.* **1989**, *111*, 7164−7175.

(23) Folkers, J. P.; Laibinis, P. E.; Whitesides, G. M. Self-Assembled Monolayers of Alkanethiols on Gold: Comparisons of Monolayers Containing Mixtures of Short and Long-chain Constituents with CH_3 and CH_2OH Terminal Groups. *Langmuir* **1992**, *8*, 1330−1341.

(24) Folkers, J. P.; Laibinis, P. E.; Whitesides, G. M.; Deutch, J. Phase Behavior of Two-Component Self- Assembled Monolayers of Alkanethiolates on Gold. *J. Phys. Chem.* **1994**, *98*, 563−571.

(25) Stranick, S. J.; Parikh, A. N.; Tao, Y.-T.; Allara, D. L.; Weiss, P. S. Phase Separation of Mixed-Composition Self-Assembled Monolayers into Nanometer Scale Molecular Domains. *J. Phys. Chem.* **1994**, *98*, 7636−7646.

(26) Smith, R. K.; Reed, S. M.; Lewis, P. A.; Monnell, J. D.; Clegg, R. S.; Kelly, K. F.; Bumm, L. A.; Hutchison, J. E.; Weiss, P. S. Phase Separation within a Binary Self-Assembled Monolayer on Au{111} Driven by an Amide-Containing Alkanethiol. *J. Phys. Chem. B* **2001**, *105*, 1119−1122.

(27) Laibinis, P. E.; Fox, M. A.; Folkers, J. P.; Whitesides, G. M. Comparisons of Self-assembled Monolayers on Silver and Gold−Mixed Monolayers Derived from $HS(CH_2)_{21}X$ and $HS(CH_2)_{10}Y$ (X, Y = CH_3, CH_2OH) Have Similar Properties. *Langmuir* **1991**, *7*, 3167−3173.

(28) Schönherr, H.; Ringsdorf, H. Self-Assembled Monolayers of Symmetrical and Mixed Alkyl Fluoroalkyl Disulfides on Gold. 1. Synthesis of Disulfides and Investigation of Monolayer Properties. *Langmuir* **1996**, *12*, 3891−3897.

(29) Schönherr, H.; Ringsdorf, H.; Jaschke, M.; Butt, H. J.; Bamberg, E.; Allinson, H.; Evans, S. D. Self-Assembled Monolayers of Symmetrical and Mixed Alkyl Fluoroalkyl Disulfides on Gold. 2. Investigation of Thermal Stability and Phase Separation. *Langmuir* **1996**, *12*, 3898−3904.

(30) Chinwangso, P.; Jamison, A. C.; Lee, T. R. Multidentate Adsorbates for Self-Assembled Monolayer Films. *Acc. Chem. Res.* **2011**, *44*, 511−519.

(31) Lee, H. J.; Jamison, A. C.; Yuan, Y.; Li, C.-H.; Rittikulsittichai, S.; Rusakova, I.; Lee, T. R. Robust Carboxylic Acid-Terminated Organic Thin Films and Nanoparticle Protectants Generated from Bidentate Alkanethiols. *Langmuir* **2013**, *29*, 10432−10439.

(32) Lee, H. J.; Jamison, A. C.; Lee, T. R. Boc-Protected ω-Amino Alkanedithiols Provide Chemically and Thermally Stable Amine-Terminated Monolayers on Gold. *Langmuir* **2015**, *31*, 2136−2146.

(33) Atre, S. V.; Liedberg, B.; Allara, D. L. Chain-Length Dependence of the Structure and Wetting Properties in Binary Composition Monolayers of OH-Terminated and CH_3-Terminated Alkanethiolates on Gold. *Langmuir* **1995**, *11*, 3882−3893.

(34) Yuan, Y.; Yam, C. M.; Shmakova, O. E.; Colorado, R., Jr.; Graupe, M.; Fukushima, H.; Moore, H. J.; Lee, T. R. Solution-Phase Desorption of Self-Assembled Monolayers on Gold Derived from Terminally Perfluorinated Alkanethiols. *J. Phys. Chem. C* **2011**, *115*, 19749−19760.

(35) Bain, C. D.; Troughton, E. B.; Tao, Y. T.; Evall, J.; Whitesides, G. M.; Nuzzo, R. G. Formation of Monolayer Films by the Spontaneous Assembly of Organic Thiols from Solution onto Gold. *J. Am. Chem. Soc.* **1989**, *111*, 321−325.

(36) Lashkor, M.; Rawson, F. J.; Preece, J. A.; Mendes, P. M. Switching Specific Biomolecular Interactions on Surfaces under Complex Biological Conditions. *Analyst* **2014**, *139*, 5400−5408.

(37) Venkataraman, N. V.; Zürcher, S.; Rossi, A.; Lee, S.; Naujoks, N.; Spencer, N. D. Spatial Tuning of the Metal Work Function by Means of Alkanethiol and Fluorinated Alkanethiol Gradients. *J. Phys. Chem. C* **2009**, *113*, 5620−5628.

(38) Ballav, N.; Terfort, A.; Zharnikov, M. Mixing of Nonsubstituted and Partly Fluorinated Alkanethiols in a Binary Self-Assembled Monolayer. *J. Phys. Chem. C* **2009**, *113*, 3697−3706.

(39) Pale-Grosdemange, C.; Simon, E. S.; Prime, K. L.; Whitesides, G. M. Formation of Self-Assembled Monolayers by Chemisorption of Derivatives of Oligo(ethylene glycol) of Structure HS-

DOI: 10.1021/acs.chemmater.6b01390
Chem. Mater. 2016, 28, 5356−5364

$(CH_2)_{11}(OCH2CH2)_mOH$ on Gold. *J. Am. Chem. Soc.* **1991**, *113*, 12−20.
(40) Harder, P.; Grunze, M.; Dahint, R.; Whitesides, G. M.; Laibinis, P. E. Molecular Conformation in Oligo(ethylene glycol)-Terminated Self-Assembled Monolayers on Gold and Silver Surfaces Determines Their Ability To Resist Protein Adsorption. *J. Phys. Chem. B* **1998**, *102*, 426−436.
(41) Porter, M. D.; Bright, T. B.; Allara, D. L.; Chidsey, C. E. D. Spontaneously Organized Molecular Assemblies. 4. Structural Characterization of *n*-Alkyl Thiol Monolayers on Gold by Optical Ellipsometry, Infrared Spectroscopy, and Electrochemistry. *J. Am. Chem. Soc.* **1987**, *109*, 3559−3568.
(42) Nuzzo, R. G.; Dubois, L. H.; Allara, D. L. Fundamental Studies of Microscopic Wetting on Organic Surfaces. 1. Formation and Structural Characterization of a Self-Consistent Series of Polyfunctional Organic Monolayers. *J. Am. Chem. Soc.* **1990**, *112*, 558−569.
(43) Bensebaa, F.; Voicu, R.; Huron, L.; Ellis, T. H.; Kruus, E. Kinetics of Formation of Long-Chain n-Alkanethiolate Monolayers on Polycrystalline Gold. *Langmuir* **1997**, *13*, 5335−5340.
(44) Shon, Y.-S.; Lee, T. R. Desorption and Exchange of Self-Assembled Monolayers (SAMs) on Gold Generated from Chelating Alkanedithiols. *J. Phys. Chem. B* **2000**, *104*, 8192−8200.
(45) Lee, S.; Shon, Y.-S.; Colorado, R., Jr.; Guenard, R. L.; Lee, T. R.; Perry, S. S. The Influence of Packing Densities and Surface Order on the Frictional Properties of Alkanethiol Self-Assembled Monolayers (SAMs) on Gold: A Comparison of SAMs Derived from Normal and Spiroalkanedithiols. *Langmuir* **2000**, *16*, 2220−2224.
(46) Srisombat, L.; Jamison, A. C.; Lee, T. R. Stability: A Key Issue for Self-Assembled Monolayers as Thin-Film Coatings and Nanoparticle Protectants. *Colloids Surf., A* **2011**, *390*, 1−19.

DOI: 10.1021/acs.chemmater.6b01390
Chem. Mater. 2016, 28, 5356−5364